THE ASTROPHYSICAL JOURNAL, 380:617–630, 1991 October 20

IRRADIATION OF ACCRETION DISKS AROUND YOUNG OBJECTS. I. NEAR-INFRARED CO BANDS

NURIA CALVET,[1,2] ALBERTO PATIÑO,[1,3] GLADIS MAGRIS C.,[1,4] AND PAOLA D'ALESSIO[5]

Received 1990 September 21; accepted 1991 April 18

ABSTRACT

We calculate in an approximate way the effect of irradiation by the central star on the atmospheres of optically thick, physically thin, accretion disks around young objects, assuming radiative equilibrium. The net effect of irradiation is to increase the temperature in the atmosphere of a viscous accretion disk relative to the case when only the viscous flux goes through it. The temperature increase at a given depth depends on the absorption and scattering coefficients characteristic of the atmosphere, and on the rate of irradiation. The effect on the near-infrared spectrum of the star-disk configuration is to decrease the strength of the absorption in the CO bands or turn them into emission, depending on the irradiation rate and on the mass accretion rate. As the stellar effective temperature increases for a given mass accretion rate, the disk surface temperature increases and the CO bands turn into emission. On the other hand, as the mass accretion rate increases for a given star, the intrinsic atmospheric (viscous) temperature increases and the effect of irradiation becomes less important; the CO bands turn then into absorption. The stellar effective temperature–disk mass accretion rate diagram can be divided into regions where the near-infrared CO bands in the spectra of young objects appear either in absorption or in emission; observed spectra of young objects such as T Tauri stars, FU Ori objects, and Herbig Be/Ae stars are in qualitative agreement with those predicted using the corresponding stellar parameters and disk mass accretion rates. This agreement suggests that the near-infrared CO bands can be used as indicators of the rate of mass accretion in the disk around young objects.

Subject headings: radiative transfer — stars: accretion — stars: pre–main-sequence

1. INTRODUCTION

In the last few years, the hypothesis of Lynden-Bell & Pringle (1974) on the existence of accretion disks around T Tauri stars (TTS) has been extensively discussed and applied to the interpretation of the spectra of these stars (see Bertout 1989, and references therein). The hypothesis has been strengthened by the fact that FU Ori events have been interpreted as the result of instabilities in the accretion disks around luminous TTS (Hartmann & Kenyon 1985, 1988; Kenyon, Hartmann, & Hewett 1988; Clarke, Lin & Pringle 1990). Also, even though their existence has not yet been clearly demonstrated, discussions on accretion disks around more massive young stellar objects have been presented (Thompson et al. 1977; Scoville et al. 1983; Thompson 1985).

Irradiation by light of the central star plays a crucial role in the heating of the outer layers of the cool disks around young objects and therefore largely determines both the continuum energy distribution and the details of the spectrum of the disk. In addition, irradiation must be included when calculating the inner disk structure, since the upper boundary conditions for the solution of the system of structure equations depends on the irradiation rate. However, the effect of irradiation has been treated very crudely so far. In most studies, the disk has been assumed optically thick and the temperature at the level where the continuum is formed has been determined from the sum of the stellar incident energy and the local viscous energy, while the details of the transfer of radiation in the disk atmosphere have been ignored (Adams, Lada, & Shu 1987; Kenyon & Hartmann 1987, hereafter KH; Bertout, Basri, & Bouvier 1988; Basri & Bertout 1989). In this approach, the detailed spectrum of the disk cannot be calculated, since it depends on the atmospheric temperature structure, which in turn is determined by the rate of deposition of stellar energy and of viscous energy in the disk's outermost layers. Nevertheless, the continuum flux from optically thick disks calculated with this assumption is in good agreement with observations. Following an alternative approach, Carr (1989) has assumed that the inner disk is optically thin and that the constant temperature at a given radius is determined from the sum of the viscous and the absorbed stellar flux. With this assumption, he calculates the near-infrared spectrum of young objects and finds that it is characterized by emission in the CO bands. However, these bands are absent or in absorption in most of the observed objects (KH; Carr 1989).

These considerations indicate that it has become important to consider in more detail the actual physical conditions in the atmospheres of irradiated optically thick disks around young objects in order to calculate the emergent spectrum of the star-disk system. In this work, we use a more accurate, but still very approximate, treatment to determine the heating of gas on the disk surface due to irradiation by a central source. We assume the disk is optically thick and determine the temperature structure of the atmospheric layers, which we define as the layers where viscous dissipation is negligible. We then calculate the emergent flux in the first-overtone bands of CO for a range of stellar effective temperatures and disk mass accretion rates. We find that for a given stellar temperature, the presence of the CO bands either in absorption or in emission is

[1] Centro de Investigaciones de Astronomía, Ap. P. 264, Mérida, 5101-A, Venezuela
[2] Also Grup d'Astrofisica de la Societat Catalana de Fisica (Institut d'Estudis Catalans)
[3] Also Departamento de Física, Universidad de Los Andes, Mérida, Venezuela.
[4] Also Universidad Central de Venezuela, Caracas, Venezuela
[5] Instituto de Astronomia, UNAM Ap. P. 70-264, 04510, Mexico D. F., Mexico; also Centro de Investigaciones de Astronomia, Merida, Venezuela

a good indicator of the mass accretion rate in the disk. The results we obtain indicate that the strength of the band could give a quantitative estimate of the mass accretion rate, but we feel that a more acccurate treatment than the one we use in this work is required to attempt this quantitative approach. After the calculation of the temperature, pressure, and extension of the atmosphere, we check if the optically thick hypothesis is consistent. This does not substitute for a detailed calculation of the inner disk structure but does give us a hint of the real physical situation. We find that for values of the α parameter of the order of 10^{-3}, as expected at least for T Tauri stars (Clarke et al. 1990), accretion disks are optically thick, in agreement with our assumption.

In § 2, we describe an approximate treatment for calculating the effect of irradiation, developed in the past for the case of close binary systems. In § 3, the application of the treatment of actual accretion disks is described, and in § 4 the results of this application are given. Finally, in § 5, we discuss the implications of our results when compared with observations.

2. MILNE-STRITTMATTER DESCRIPTION FOR THE EFFECT OF IRRADIATION

We consider the problem of irradiation on the disk atmosphere in a very idealized way, following the treatment of superposition of solutions used by Milne (1930) to estimate the reflection effect in eclipsing binaries. We consider a semi-infinite mass of material with plane-parallel symmetry (this assumption implies that the disk is optically thick) exposed to incident radiation on the boundary. We assume steady state and radiative equilibrium. We assume there is a constant net flux F_v generated in the interior of the disk which is transported through the atmosphere to space. The incident radiation alters the temperature structure in the outer, low–optical depth layers relative to the case with no irradiation, in such a way that all the energy incident on the boundary of those layers is radiated back. This is Milne's reflection effect. In the case of LTE, when the source function is determined by local conditions, the transfer equation is linear in the specific intensity I, and solutions can be superposed. Then, if $T_1(\tau)$ is the temperature distribution that gives net flux F_v with boundary condition of zero incident radiation, and $T_2(\tau)$ is a temperature distribution with incident radiation equal to a given value but with zero net flux (reflection effect), then the distribution $T(\tau)$ such that $T^4 = T_1^4 + T_2^4$ corresponds to the case with net flux equal to F_v and incident radiation equal to its given value. We take the solution $T_1(\tau)$ as that of a constant flux, gray atmosphere in the Eddington approximation, $T_1^4(\tau) = 3/4F_v\ (\tau + 2/3)$, with $\tau = -\int \chi_{\rm Ross}\rho\, dz$, $\chi_{\rm Ross}$ being the Rosseland mean opacity and ρ the density, and estimate $T_2(\tau)$.

We approach the problem of calculating $T_2(\tau)$ in a way similar to that used by Strittmatter (1974) to estimate the effect of heating by X-rays on the atmosphere of the companion in the close binary system HZ Her. The treatment is not so appropriate here as it is for systems as HZ Her, since in this latter case, the frequency range where the atmosphere is heated, the X-rays, and that where the atmosphere emits, the optical, are well separated in energy, so that no intrinsic emission from the atmosphere is expected at X-ray wavelengths. In some cases treated here, the atmospheric surface temperature is comparable to the stellar effective temperature, so some stellar photons are being absorbed in the frequency region where there is some intrinsic emission from the disk. In any event, the motivation of this investigation is to estimate the size of the effects which results from including physical constraints that have been ignored in the treatments done so far. If these effects prove to be important, then a more accurate treatment of the problem will be justified.

We will describe here Strittmatter's treatment, following Milne's explanation for the sake of clarity. The incident radiation consists of a parallel beam carrying energy E_0 (ergs cm^{-2} s^{-1}) per unit area normal to itself, incident at an angle $\cos^{-1}\mu_0$ from the normal to the boundary of the (plane-parallel) atmosphere. This incident beam is absorbed as it penetrates the material. A fraction σ of the energy in the beam will be scattered, that is, it will remerge at the same frequency range as that of the incident beam, creating a diffuse field I_s. A fraction α of the incident beam will be truly absorbed and reemitted at frequencies determined by the temperature of the gas. As the characteristic kinetic temperature of the atmosphere is lower than the radiation temperature characterizing the incident radiation, we will assume that no true emission occurs in the frequency range where the stellar radiation is significant and that no scattering of radiation from the incident beam occurs in the frequency range where the true emission is significant. We call these two frequency ranges in a loose sense as disk (d) and stellar (s) and assume that the atmospheric opacities are approximately constant in each. The parameters α and σ are constant in the atmosphere. For the description below, we follow Mihalas's (1978) notation.

The flux of radiation incident in the boundary per unit area is $E_0\mu_0$. This beam is absorbed exponentially as it penetrates the material, so at optical depth τ_s the energy contained in the beam per unit area parallel to the surface is

$$E_0\mu_0 e^{-\tau_s/\mu_0}\,. \tag{1}$$

The absorption of the incident beam in $d\tau_s$ at depth τ_s is

$$E_0\mu_0 e^{-\tau_s/\mu_0}\, d\tau_s/\mu_0 = E_0 e^{-\tau_s/\mu_0}\, d\tau_s\,. \tag{2}$$

Of this energy absorbed in $d\tau_s$, we assume that a fraction σ will be scattered, so we can write the equation of transfer for the radiation I_s as

$$\mu\frac{dI_s}{d\tau_s} = I_s - \frac{\sigma E_0 e^{-\tau_s/\mu_0}}{4\pi} - \frac{\sigma\int I_s\, d\omega}{4\pi}\,, \tag{3}$$

where we assume the radiation field at this frequency range is described by the diffuse field I_s, for $\mu \neq \mu_0$, and by the incident field for $\mu = \mu_0$.

Taking the moments of equation (3) and using the Eddington approximation, we get

$$J_s = \frac{\mu_0\sigma E_0(2+3\mu_0)}{4\pi[1+(2\beta/3)](1-\beta^2\mu_0^2)}\, e^{-\beta\tau_s} - \frac{3\mu_0^2\sigma E_0}{4\pi(1-\beta^2\mu_0^2)}\, e^{-\tau_s/\mu_0} \tag{4}$$

and

$$H_s = -\frac{\mu_0\sigma E_0\beta(2+3\mu_0)}{12\pi[1+(2\beta/3)](1-\beta^2\mu_0^2)}\, e^{-\beta\tau_s} + \frac{\mu_0\sigma E_0}{4\pi(1-\beta^2\mu_0^2)}\, e^{-\tau_s/\mu_0} \tag{5}$$

where $\alpha = 1-\sigma$, $\beta = (3\alpha)^{1/2}$ and where the boundary condition, $J_s(0) = 2H_s(0)$, has been used for the radiation field I_s.

The condition of zero net flux can be written as

$$H = H_s + H_d = E_0\mu_0 e^{-\tau_s/\mu_0}/4\pi \tag{6}$$

that is, the emergent flux, H, is equal to the incident flux. From equations (6) and (5),

$$H_d = H_0 \mu_0 \alpha[(1 + C_1)e^{-\tau_s/\mu_0} + C_2 e^{-\beta\tau_s}] \quad (7)$$

where $H_0 = E_0/4\pi$,

$$C_1 = -\frac{3\sigma\mu_0^2}{1 - \beta^2\mu_0^2} \quad (8)$$

and

$$C_2 = \frac{\sigma(2 + 3\mu_0)}{\beta[1 + (2\beta/3)](1 - \beta^2\mu_0^2)} \quad (9)$$

The transfer equation for the diffuse radiation field at the frequency range determined by the local temperature, according to our assumptions, can be written as

$$\mu \frac{dI_d}{d\tau_d} = I_d - B . \quad (10)$$

From the first moment of equation (10),

$$B = \frac{\sigma_R T_2^4}{\pi} = J_d - \frac{dH_d}{d\tau_d} . \quad (11)$$

From the second moment of equation (10), using equation (7) and the Eddington approximation,

$$J_d = H_0 \mu_0 \alpha[(1 + C_1)(2 + 3\mu_0/q) + C_2(2 + 3/\beta q) - 3\mu_0/q(1 + C_1)e^{-q\tau_d/\mu_0} - 3C_2/\beta q e^{-\beta q\tau_d}] , \quad (12)$$

where

$$q \equiv \tau_s/\tau_d . \quad (13)$$

The temperature structure for the zero net flux case can then be obtained by use of equations (7) and (12) in equation (11).

The temperature structure corresponding to an atmosphere that has net flux equal to F_v and incident radiation of flux $E_0\mu_0$ at the surface is, according to the considerations at the beginning of the section,

$$T^4(\tau_d) = \frac{3}{4} T_v^4\left(\tau_d + \frac{2}{3}\right) + \frac{\alpha E_0 \mu_0}{4\sigma_R} \times [C_1' + C_2' e^{-q\tau_d/\mu_0} + C_3' e^{-\beta q\tau_d}] , \quad (14)$$

where

$$C_1' = (1 + C_1)\left(2 + \frac{3\mu_0}{q}\right) + C_2\left(2 + \frac{3}{\beta q}\right) \quad (15)$$

$$C_2' = \frac{(1 + C_1)}{\mu_0}\left(q - \frac{3\mu_0^2}{q}\right) \quad (16)$$

and

$$C_3' = C_2\beta\left(q - \frac{3}{q\beta^2}\right) , \quad (17)$$

where $T_v = (F_v/\sigma_R)^{1/4}$. For $q \to 1$ and $\sigma = 0$, this equation reduces to

$$T^4(\tau_d) = \frac{3}{4} T_v^4\left(\tau_d + \frac{2}{3}\right) + \frac{E_0}{4\sigma_R}[\mu_0(2 + 3\mu_0) + (1 - 3\mu_0^2)e^{-\tau_d/\mu_0}] \quad (18)$$

which is Milne's case, solved in the Eddington approximation.

3. APPLICATION TO THE STAR-DISK SYSTEM

We consider a star of effective temperature T_*, mass M_*, and radius R_*, surrounded by a steady, viscous, geometrically thin, optically thick accretion disk. The disk accretes material onto the star at a rate $\dot{M}_a$ and has height H which varies with distance r from the center of the star. We assume that the outer layers of the disk form an atmosphere through which the viscous flux generated in the dense disk interior is transported, with no additional generation of energy. If only the viscous flux is considered in the gray approximation, the effective disk temperature at distance r from the star, $T_v(r)$, is equal to $(F_v/2\sigma_R)^{1/4}$, where the viscous flux F_v is given by

$$F_v = \frac{3GM_*\dot{M}_a}{4\pi r^3}\left[1 - \left(\frac{R_*}{r}\right)^{1/2}\right] \quad (19)$$

(Shakura & Sunyaev 1973).

If, in addition to the viscous flux, we consider the irradiation of light from the central star at each radius of the disk, the atmospheric temperature is altered in a way that can be approximately described by the treatment outlined in § 2. The temperature structure is characterized by constant parameters q and α in that treatment, but in the actual atmosphere the opacity is wavelength-dependent and changes as pressure and temperature vary. In addition, the incoming radiation is assumed to be a parallel beam, while in the star-disk case, the two components are so close that the incoming light enters the disk with a finite range of angles. We have then to devise a method to calculate appropriate mean values for these parameters to apply the Milne-Strittmatter treatment.

3.1. *Estimate of q and α*

To estimate values of q and α appropriate for characterizing the disk atmosphere, we need to know first the opacity as a function of temperature and density. We have not carried out a complete analysis of the molecular opacity sources, which would require a detailed treatment of millions of lines, since it is unwarranted by our other approximations. We have included the following components in the opacity calculations: (1) H bound-free and free-free; (2) H^- bound-free and free-free; (3) H_2^+; (4) C, Si, and Mg. For components (1)–(4), we have used routines from Carbon & Gingerich (1969); (5) He^- free-free using a fit by Gray (1976) to the results of McDowell, Williamson, & Myerscough (1966); (6) Rayleigh scattering of H and He from Dalgarno (1962) and H_2 from Vardya (1962); (7) electron scattering; (8) fundamental and first-overtone bands of the vibrational-rotational transitions of the electronic ground state of CO, from tables in Kirby-Docken & Liu (1978), using partition functions from Tatum (1966). Pure rotational band of CO from Tsuji (1966); (9) α, γ, and ϕ systems of TiO from Collins & Fay (1974), with electronic oscillator strengths from Tsuji (1969); (10) fundamental and first-overtone bands of the electronic ground state and pure rotational band of OH from Tsuji (1966), in the just-overlapping approximation; (11) H_2^- free-free from Tsuji (1966), with the approximation $\kappa(H_2^-) = 0.2\kappa(H^-)$ for $T < 1400$ K; (12) red and infrared bands of H_2O, interpolating in temperature in tables from Auman (1967). For temperatures out of the range covered by Auman's tables, the opacity was taken equal to that of the highest or lowest temperature in the tables, if the temperature was higher or lower than the limits, respectively, with continuum opacity calculated at the local temperature; the pure rotational transition is from Tsuji (1966); (13) silicate and

graphite grains, using abundances appropriate for the interstellar medium and a grain size distribution proportional to $a^{-3.5}$, and grain sizes from $a = 0.005$ to $a = 0.3$ μm, as in Draine & Lee (1984), with grain properties from Draine (1987). We assume that grains are destroyed above 1500 K.

Atomic and molecular populations were calculated using the same procedure and molecular constants as Kurucz (1970). For TiO, the dissociation constant was taken from Tatum (1966). We assume LTE and that the kinetic temperature characterizes all distributions, which is an appropriate approximation since densities are $\geq 10^{11}$ cm^{-3}. Below 900 K, all material is assumed to be molecular hydrogen. The turbulent velocity was fixed at the local sound velocity. Tables of the Rosseland mean opacity were calculated using these opacity sources, with an abundance similar to the King Va mixture of Alexander (1975). In the temperature range between 1500 and 3000 K, the calculated Rosseland mean opacity is lower than the corresponding opacity in Alexander (1975), agrees well with the improved calculations of Alexander, Johnson, & Rypma (1983), but is higher than that in Alexander, Augason, & Johnson (1989), calculated with an opacity-sampled treatment for water vapor. The resultant temperature profiles are then cooler at given mass column density than those that would be obtained with this latter treatment for the water opacity (Alexander et al. 1989). The continuum level around the CO bands, on the other hand, which depends mostly on the water opacity, is well determined for a given temperature structure, since the water opacity of Auman (1967) agrees well with the laboratory data of Ludwig et al. (1974) at ≈ 2.3 μm.

To estimate q, we first need to know the mean opacity in the wavelength range at which the stellar radiation is absorbed and the mean opacity characterizing the atmosphere. To estimate the second, we take the Rosseland mean opacity of the gas. For the first, we calculate the mean of the inverse of the opacity, weighted by the derivative of the Planck function evaluated at the stellar temperature, for a gas of given temperature and pressure. In this way, a similar mean is taken in both cases. We take q for the given temperature and pressure as the ratio of these two quantities. For estimating α, we take the mean of α_ν, weighted by the Planck function evaluated at the stellar temperature. Figures 1*a* and 1*b* show q and α as a function of temperature for several pressures and for stellar temperatures $T_* = 4000$, 5000, and 10,000 K. For a given pressure, q approaches unity as T tends to the stellar temperature, as it should by definition, then reaches a maximum as T decreases, and decreases again. The temperature at which the maximum in q occurs decreases as the pressure decreases. At the temperature of the maximum, the opacity in the "stellar" frequency band is due mostly to Rayleigh scattering by neutral H, while no opacity source of comparable strength exists at longer wavelengths, because there is no significant population of molecules. This is apparent in the curves for α in Figure 1*b*. As the temperature decreases, molecular opacity becomes more important in all wavelength regions and q decreases. The prevalence of molecular opacity occurs at higher temperatures as the pressure increases, which explains the shift of the maximum with pressure. For $T < 2000$ K, curves for all pressures converge into one, because all the material available is locked into molecules. The abrupt jump at 1500 K is due to our unrealistic hypothesis that grains are suddenly destroyed at that temperature, so that the opacity jumps from the high dust opacity in the low temperature side to the molecular opacity in the high temperature side. Note that the value of q for a given temperature and pressure increases as T_* increases, due to the fact that the peak of the stellar energy shifts to shorter wavelengths, where the opacity, either scattering or dust, is higher.

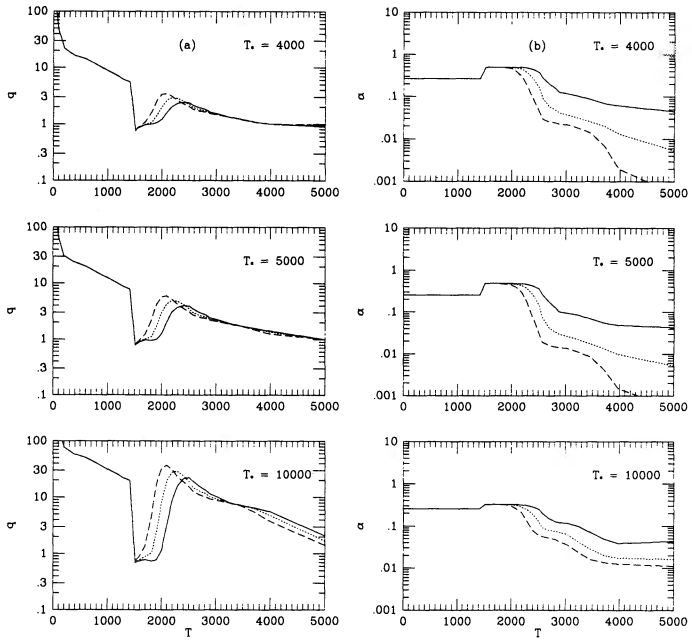

FIG. 1.—Parameters (*a*) q and (*b*) α as a function of temperature. *Continuous line*: $\log p = 0$; *dotted line*: $\log p = -1$; *dashed line*: $\log p = -2$.

We use for the atmospheric calculations the values of q and α evaluated at the temperature and pressure of the surface, at points where $\tau \ll 1$ and where the temperature has already reached its asymptotic value. To do this, we take a value of the pressure, p_0, and solve equation (14), evaluated at $\tau = 0$, as an implicit equation for $T(\tau = 0) = T_0$. We use $q(T_0, p_0)$ and $\alpha(T_0, p_0)$ for the rest of the atmosphere. The value of p_0, which we take as characteristic of the outermost layers, is estimated by trial and error, calculating atmospheric structures with q evaluated at different pressures, and selecting the one that gave superficial pressures consistent with the value assumed for calculating q. The assumed values of p_0 are given in Table 1. The drop in the value of p_0 in the outer radii of the low stellar temperature cases is due to the fact that the temperature at those radii is $\lesssim 1500$ K, so that the opacity due to dust is high and for a given mass column density the optical depth is larger than in the hotter atmospheres. For regions with $1500 < T < 2000$ K, the actual value of the temperature is sensitive to the adopted value of p_0, especially around the region $T \approx 1500$ K, where the opacity jumps. An iterative scheme for estimating T_0 and p_0 does not give good results, since the present treatment has no means of enforcing convergence. The sensitivity to the value of p_0 can introduce differences up to 400 K in the surface temperature; fortunately, at these temperatures the contribution to the flux in the CO bands is small, and the resultant fluxes are not largely affected by this uncertainty.

3.2. *Calculation of* μ_0 and E_0

To define the average values of μ_0 and E_0 characterizing the incoming radiation, we take at each radius the mean of the cosine of the incidence angle and of the intensity of the stellar surface from which it is emitted. We adopt the geometry of

TABLE 1

ADOPTED VALUES OF SURFACE PRESSURE

	T_* (K)								
	4000			5000			10000		
r/R_*	$\dot{M}_a = 10^{-8}$	10^{-7}	10^{-6}	$\dot{M}_a = 10^{-8}$	10^{-7}	10^{-6}	$\dot{M}_a = 10^{-8}$	10^{-7}	10^{-6}
1.5	1	2	4	6	6	5	2	2	1
2	0.08	0.2	4	4	4	5	4	4	2
3	0.001	0.001	0.3	0.2	0.4	2	2	2	2
4	0.001	0.001	0.03	0.05	0.1	0.2	1	1	1
5	0.001	0.001	0.001	0.05	0.005	0.005	1	1	1
6	0.001	0.001	0.001	0.001	0.001	0.001	1	1	1
7	0.001	0.001	0.001	0.001	0.001	0.001	1	1	1
8	0.001	0.001	0.001	0.001	0.001	0.001	1	1	0.9
9	0.001	0.001	0.001	0.001	0.001	0.001	0.9	0.9	0.8
10	0.001	0.001	0.001	0.001	0.001	0.001	0.8	0.8	0.7

[a] Pressure in dyn cm^{-2}.

KH. To solve the problem properly, we would have to calculate the inner disk structure consistent with the surface temperature structure resultant from irradiation. That is, we would have to solve the set of internal structure equations, using as upper boundary condition for the temperature the value given by equation (14) evaluated at $\tau = \frac{2}{3}$. This boundary condition, in turn, would depend on the height of the disk through the parameters μ_0 and E_0, which is a result of the disk structure calculations. The problem is of a higher degree of sophistication than that of the treatment of the effects of irradiation developed here, so that we have not solved it. Instead, we have assumed, following KH, that

$$H = H_0\left(\frac{r}{R_*}\right)^{\zeta} \tag{20}$$

where we use $\zeta = 9/8$, which corresponds to the approximate variation of scale height with radius expected from a steady accretion disk. With this approximation, the values of μ_0 and E_0 can be readily calculated. The value of H_0 has been taken as 0.1 the stellar radius.

3.3. CO *Opacity*

The values for the wavenumbers and oscillator strengths for the first-overtone bands of the vibrational-rotational transitions of the electronic ground state of CO have been taken from the compilation of Kirby-Docken & Liu (1978). For each line we take a Doppler profile, which is appropriate for densities less than 10^{16} cm^{-3}, and include microturbulence in the Doppler width calculation. Microturbulence has been set at the local sound velocity.

3.4. *Model Atmosphere*

Given $T(\tau)$ as specified by equation (14), with optical depth calculated with the Rosseland mean opacity, we solve the hydrostatic equilibrium equation for the pressure

$$\frac{dp}{d\tau} = \frac{GM_*H}{r^3}\frac{(1 + z/H)}{\{1 + [(z + H)^2/r^2]\}^{3/2}}\frac{1}{\chi_{\rm Ross}} \equiv \frac{g(z)}{\chi_{\rm Ross}} \tag{21}$$

together with

$$\frac{dz}{d\tau} = -\frac{1}{\chi_{\rm Ross}\rho} \tag{22}$$

where z is the height of the atmosphere over the level where $\tau = \frac{2}{3}$. By solving this system, we include also the case in which the extent of the atmosphere is not negligible compared to H. We solve it by iteration, using in each iteration the values of $z(\tau)$ obtained in the previous one, until the difference in the value of $p(\tau)$ in successive iterations is smaller than a fixed bound. The calculation of the density ρ includes 16 elements in three ionization stages and 13 molecular species, including all the ones in Mihalas (1967). LTE is assumed.

3.5. *Optical Depth of the Disk*

In this analysis, we cannot determine the total optical depth of the disk. To do so, we would have to calculate an internal structure for the disk that fulfilled the structure equations and that matched the atmospheric parameters at $\tau = \frac{2}{3}$. Only after doing that, if that structure could be found, could we ensure that the disk was optically thick. Instead, here we assume that the disk is thick, and calculate the outer structure of the configuration which corresponds to optical depths in the continuum from 0 to 5. We assume that this region is so thin that no energy dissipation occurs and the flux is constant. In an accretion disk, the flux due to viscous dissipation is zero at the midplane of the disk, and has a gradient given by

$$\frac{dF_v}{d\tau} = -1.5\frac{\alpha_v\Omega p}{\chi_{\rm Ross}\rho}. \tag{23}$$

Here α_v is the viscosity parameter, and $\Omega(r)$ is the rotational angular velocity (Shakura & Sunyaev 1973). To check if the hypothesis of constant flux is fulfilled, after the model atmosphere is obtained, we calculate the value of the viscous flux, integrating equation (23) from $\tau = 0$, with boundary condition (19). If the flux in the atmosphere is not constant, that is, if it decreases as the height decreases, then that means that the midplane of the disk is approached and still the optical depth is less than 5, or in other words, that the disk is optically thin. We have used this criterion to explore the possibility of having optically thin or optically thick (inner) disks in the plane ($\dot{M}_a$, α_v) for different values of T_*.

3.6. *Emergent Flux*

The disk was divided into annuli, and in each one monochromatic intensity calculations were performed, using the opacity sources listed in § 3.1 and the hypothesis of LTE for the source function. Each annulus was divided into 50 angles and the flux was calculated adding the contribution from each

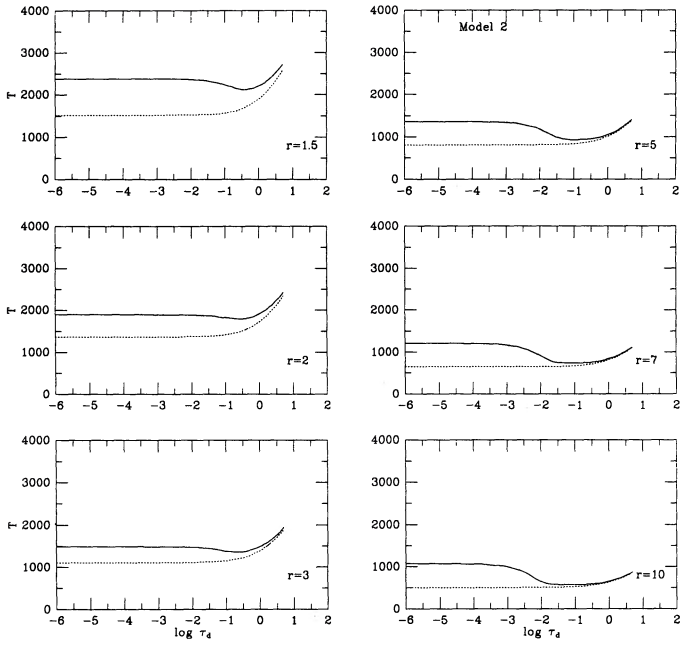

FIG. 2a

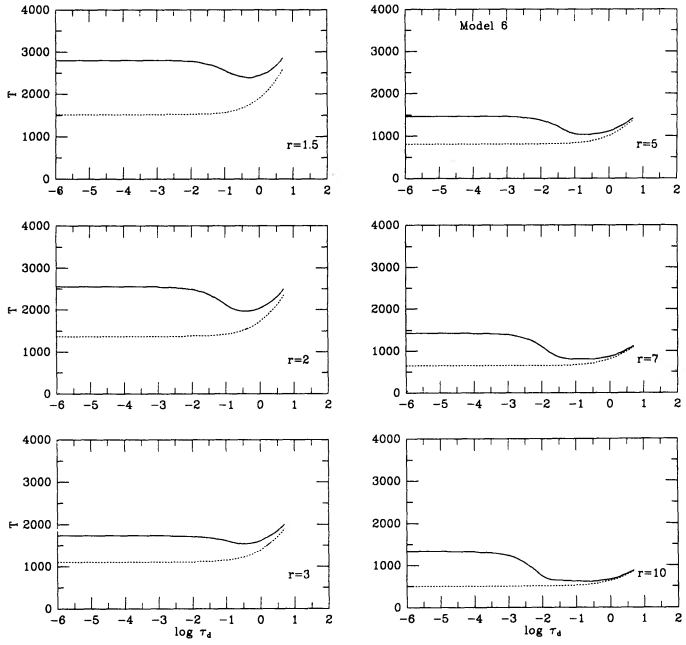

FIG. 2b

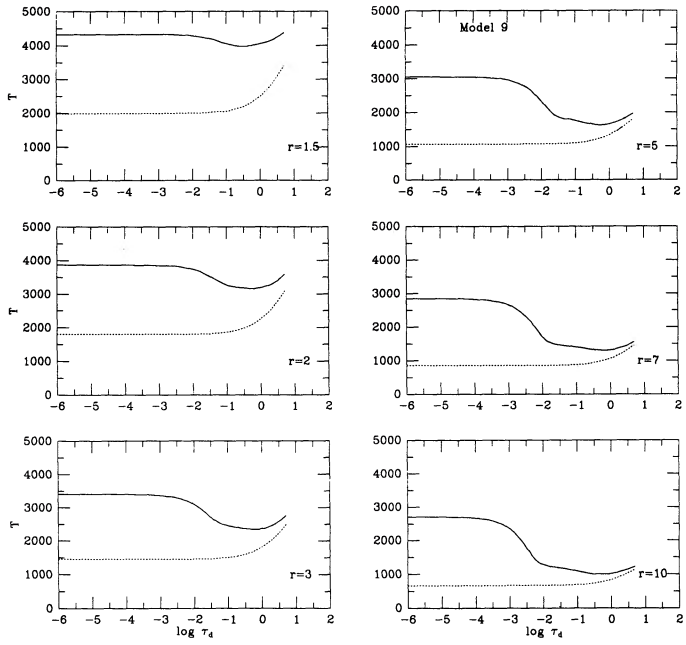

FIG. 2c

FIG. 2.—Atmospheric temperature profile $T(\tau_d)$ at several positions in the disk for models with $\dot{M}_a = 10^{-7}\ M_\odot\ \mathrm{yr}^{-1}$ and increasing T_* in Table 2: (*a*) Model 2; (*b*) Model 6; (*c*) Model 9. The radius r is in units of the stellar radius. The dotted line shows the temperature profile when no irradiation is present.

angular portion shifted apppropriately in wavelength according to the component of its orbital velocity along the line of sight. A Keplerian velocity law was assumed for the disk. The flux of the system was calculated adding the contribution from all the annuli until some maximum radius, and the contribution from the star, correcting for occultation by the disk. The maximum radius for the calculations was taken as to include the portion of the disk that contributes the most to the flux in the region around 2.3 μm. It generally was assumed to be $10R_*$, but in the cases with $T_* = 10{,}000$ K and for model 4 ("FU Ori"), the calculation was extended to $30R_*$ and to $60R_*$, respectively.

For the stellar flux, we have calculated the flux produced by a photosphere with structure similar to models with $T_{\rm eff} = 4000$ K, 5000 K and 10,000 K, all with $\log g = 4$, from Carbon & Gingerich (1969). Neither microturbulence nor stellar limb darkening have been included in the photospheric structure or flux calculations.

4. RESULTS

4.1. *Temperature Structure*

The effect of irradiation by the central star on the atmospheric structure of the disk is to alter the temperature of the outermost layers, increasing it above the value it would have if only the viscous flux was going through those layers. The details of the resultant temperature profile, for given mass accretion rate, depend on the characteristics of the incoming radiation, E_0 and μ_0, and specially on the local parameters that determine the transfer of radiation, q and α. In general, the temperature distribution is characterized by an initial decrease with height at the deepest atmospheric levels, a temperature minimum, and a rise to flatten up in a plateau in the higher layers. Here, we consider the parameters relevant to the formation of strong spectral features in LTE, namely, the temperature of the plateau or surface temperature, T_0, and the temperature at the level where the continuum forms, $T_{\rm eff}$. Table 3 gives for models in Table 2, the values of T_0, $T_{\rm eff}$, and the viscous temperature at $\tau = \frac{2}{3}$, $T_{\rm vis}$. Illustrative temperature profiles $T(\tau_d)$ at several disk radii for models 2, 6, and 9 in Table 2 are shown in Figure 2. These models correspond to disks with $\dot{M}_a = 10^{-7}\ M_\odot\ \mathrm{yr}^{-1}$, irradiated by stars of different effective temperatures. For comparison, the dashed line shows the viscous temperature profile, that is, the temperature the atmosphere would have with no irradiation. Figure 3 shows the run of T_0, q, and α for cases in Figure 2.

Examination of Table 3 shows that the ratio $T_0/T_{\rm eff}$ is larger

TABLE 2

CALCULATED MODELS

Number	$M_*(M_\odot)$	$R_*(R_\odot)$	T_*(K)	$\dot{M}_a(M_\odot\ \mathrm{yr}^{-1})$	Comment
1.....	1	3	4000	10^{-8}	
2.....	1	3	4000	10^{-7}	
3.....	1	3	4000	10^{-6}	
4.....	1	3	4000	10^{-4}	FU Ori
5.....	1	3	5000	10^{-8}	
6.....	1	3	5000	10^{-7}	
7.....	1	3	5000	10^{-6}	
8.....	3	3	10000	10^{-8}	
9.....	3	3	10000	10^{-7}	
10.....	3	3	10000	10^{-6}	
11.....	3	3	10000	10^{-5}	
12.....	1	3	4000	10^{-8}	Boundary layer (see text)
13.....	1	3	4757	10^{-8}	Boundary layer (see text)

than 1 at all radii considered at low mass accretion rates, reflecting the predominance of the irradiation terms in equation (14). As $\dot{M}_a$ increases, the value of $T_{\rm eff}$ increases, becoming more similar to the value of $T_{\rm vis}$. The surface temperature also increases, but at a slower rate, so that above some value of $\dot{M}_a$ for given stellar parameters, $T_0/T_{\rm eff}$ approaches the value 0.84, appropriate to the gray temperature law. The ratio $T_0/T_{\rm eff}$ becomes less than 1 first for the inner disk radii, for given stellar parameters. The reason for that is that the irradiation terms become more important as radius increases. To see this, consider the ratio $T_{\rm vis}/(E_0\,\mu_0)^{1/4}$, which gives a measure of the importance of the viscous term over the irradiation term in equation (14). From equation (19), $T_{\rm vis} \propto r^{-3}$. If the disk were flat, then $\mu_0 \propto r^{-1}$ and $E_0\,\mu_0 \propto r^{-3/4}$. However, the flaring of the disk implies that $\mu_0 \propto r^{-\gamma}$ with $\gamma < 1$ (KH). Therefore, $T_{\rm vis}/(E_0\,\mu_0)^{1/4} \propto r^{-(1-\gamma)/4}$, showing the increasing importance of irradiation for larger radii.

Consider the case in which the viscous terms are negligible.

TABLE 3

CHARACTERISTIC TEMPERATURES IN THE DISK ATMOSPHERE

		T_*(K)											
		4000				5000				10000			
$\dot{M}_a$	r/R_*	$T_{\rm vis}$	$T_{\rm eff}$	$T_{\rm rep}$	T_0	$T_{\rm vis}$	$T_{\rm eff}$	$T_{\rm rep}$	T_0	$T_{\rm vis}$	$T_{\rm eff}$	$T_{\rm rep}$	T_0
10^{-8}.....	1.5	1013	1854	2124	2322	1013	2205	2635	2777	1333	3896	5245	4298
	2	917	1531	1699	1703	917	1751	2096	2530	1207	3002	4162	3847
	3	742	1075	1258	1460	741	1362	1543	1646	976	2170	3052	3390
	4	623	836	1019	1419	623	1059	1248	1485	820	1746	2463	3196
	5	541	703	866	1328	541	873	1057	1458	711	1463	2085	3052
	6	480	615	759	1248	480	746	925	1441	631	1277	1822	2914
	7	433	547	676	1190	433	651	823	1426	569	1114	1620	2841
	8	395	498	613	1137	395	580	746	1414	520	1046	1468	2787
	9	365	455	560	1097	365	529	680	1369	480	946	1337	2743
	10	339	421	519	1058	339	489	630	1321	446	803	1239	2700
10^{-7}.....	1.5	1801	2151	2337	2382	1801	2395	2755	2803	2370	4015	5294	4327
	2	1631	1847	1958	1896	1631	1991	2252	2551	2146	3164	4226	3864
	3	1319	1429	1512	1486	1319	1567	1702	1729	1736	2347	3122	3400
	4	1109	1170	1250	1431	1109	1277	1395	1494	1459	1916	2529	3203
	5	962	1004	1074	1359	962	1080	1192	1464	1265	1628	2146	3056
	6	853	887	948	1269	853	943	1049	1444	1123	1385	1879	2919
	7	769	798	851	1207	769	839	938	1429	1013	1208	1673	2843
	8	703	727	775	1151	703	760	853	1415	925	1135	1518	2788
	9	648	670	712	1108	648	697	781	1374	853	1021	1384	2744
	10	603	622	661	1068	603	647	725	1326	794	851	1283	2700
10^{-6}.....	1.5	3202	3274	3340	2859	3202	3355	3513	3063	4214	4777	5718	4468
	2	2900	2938	2976	2601	2900	2980	3074	2799	3817	4133	4753	4095
	3	2345	2364	2387	2139	2345	2388	2443	2418	3087	3258	3646	3592
	4	1971	1987	2001	1754	1971	2006	2042	1893	2594	2713	3006	3269
	5	1710	1720	1733	1509	1710	1739	1765	1616	2250	2340	2580	3101
	6	1517	1524	1537	1433	1517	1539	1563	1485	1997	2070	2274	2961
	7	1368	1374	1385	1358	1368	1384	1408	1454	1801	1862	2039	2859
	8	1250	1255	1265	1273	1250	1260	1285	1432	1645	1699	1857	2794
	9	1153	1156	1166	1211	1153	1163	1184	1417	1518	1565	1705	2736
	10	1072	1075	1084	1155	1072	1081	1100	1374	1411	1456	1583	2681

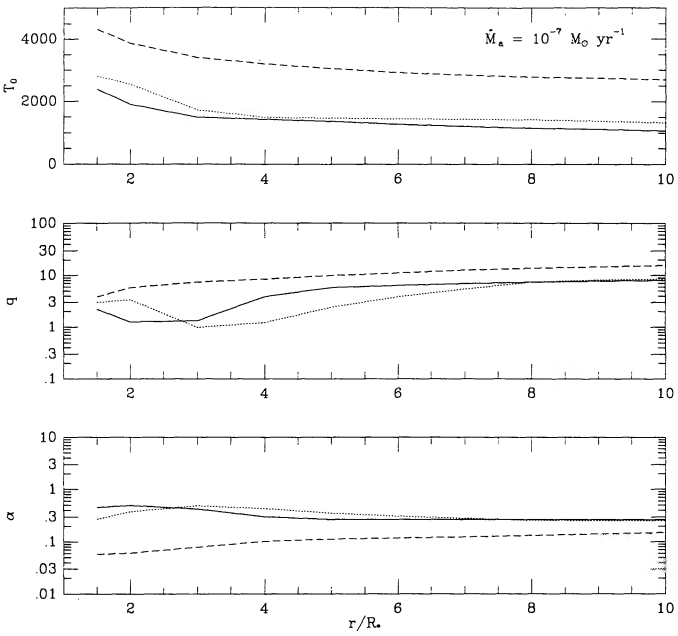

FIG. 3.—Surface temperature and parameters q and α as a function of radius for models with temperature profiles shown in Fig. 2. *Continuous line:* model 2; *dotted line*: model 6; *dashed line*: model 9.

From equation (19), the surface temperature is given by

$$T_0^4 = \frac{\alpha E_0 \mu_0}{4\sigma_R}\left[\frac{q}{\mu_0}(C_1 + 1) + \beta q C_2 + 2(C_1 + C_2 + 1)\right] \quad (24)$$

while the effective temperature is

$$T_{\rm eff}^4 = \frac{\alpha E_0 \mu_0}{4\sigma_R}\left[(1 + C_1)\left(2 + \frac{3\mu_0}{q}\right) + C_2\left(2 + \frac{3}{\beta q}\right) + \frac{(1 + C_1)}{\mu_0}\left(q - \frac{3\mu_0^2}{q}\right)e^{-2q/3\mu_0} + C_2\beta\left(q - \frac{3}{q\beta^2}\right)e^{-2\beta q/3}\right]. \quad (25)$$

Calculations show that $C_1 \ll 1$ and $C_2 \approx 1$. Since $\mu_0 \ll 1$, the most important term in the right-hand side of the expression for T_0 is the first one within the square brackets, so that $T_0^4 \approx \alpha E_0 q/4\sigma_R$. On the other hand, in the expression for $T_{\rm eff}$, the terms with exponentials in the right-hand side are ≈ 0, since $\mu_0 \ll 1$ and β and $q \gtrsim 1$, so that $T_{\rm eff}^4 \approx (\alpha E_0 \mu_0/2\sigma_R)(1 + C_2) \approx \alpha E_0 \mu_0/\sigma_R$. Therefore, for the parameters appropriate to the type of disks considered in this work and in the case that viscous terms can be neglected, $T_0/T_{\rm eff} \approx (q/4\mu_0)^{1/4}$, which reflects the fact that for increasing q and a more oblique incidence of the stellar ray, an increasing fraction of the energy is deposited in the outermost layers. Since $q \gtrsim 1$ and $\mu_0 \ll 1$, the ratio $T_0/T_{\rm eff} > 1$ when irradiation dominates, as happens for all radii at low mass accretion rates.

Table 3 also gives the value of

$$T_{\rm rep} = (T_{\rm vis}^4 + E_0 \mu_0/\sigma_R)^{1/4} \quad (26)$$

which is the value of the effective temperature obtained under the assumption used so far in calculating the flux from reprocessing disks (Adams et al. 1987; KH; Bertout et al. 1988), namely, that the energy emitted by the star is absorbed at $\tau = \frac{2}{3}$. This value is obtained from equation (25) if q is small and $\alpha = 1$. Figure 4 shows the value of $T_{\rm eff}$, $T_{\rm vis}$, and $T_{\rm rep}$ as a function of radius for mass accretion rates $\dot{M}_a = 10^{-7}$ and 10^{-8} $M_\odot$ yr^{-1}, and $T_* = 4000$ K, 5000 K, and 10,000 K (other stellar parameters as in Table 2). In all cases, the value of the effective temperature is higher than that of the viscous temperature, but it is still below the value which has been assumed in the reprocessing disk calculations. The implications of this result for the continuum fluxes and the disk will be discussed elsewhere (Calvet et al. 1991).

4.2. *Validity of the Assumptions Used*

To obtain the temperature structure given by equation (14) from which the main results of this work follow, we have made several simplifying assumptions: (1) the atmosphere is gray, (2) the Eddington approximation holds, (3) the stellar radiation is absorbed in a frequency range where there is no intrinsic emission from the atmosphere, (4) the values of q and α that are valid at the surface are valid throughout the atmosphere, (5) no convection is present, and (6) radiative equilibrium (RE) holds. These assumptions are in general inadequate, as we will shortly review, and the justification for using them is the exploratory nature of this work. At the temperatures considered, molecules provide the dominant source of opacity, which is far from gray. The hypothesis of isotropy, implicit in the Eddington approximation, is likely not valid in the low-density regions near the boundary. Atmospheric surface temperatures are of the same order as the stellar temperature for the low irradiation cases, so $q \approx 1$, where the treatment is more uncertain. Moreover, q and α change significantly with temperature and pressure, so conditions at the surface differ from those at deep atmospheric levels.

We have determined stability against convection by compar-

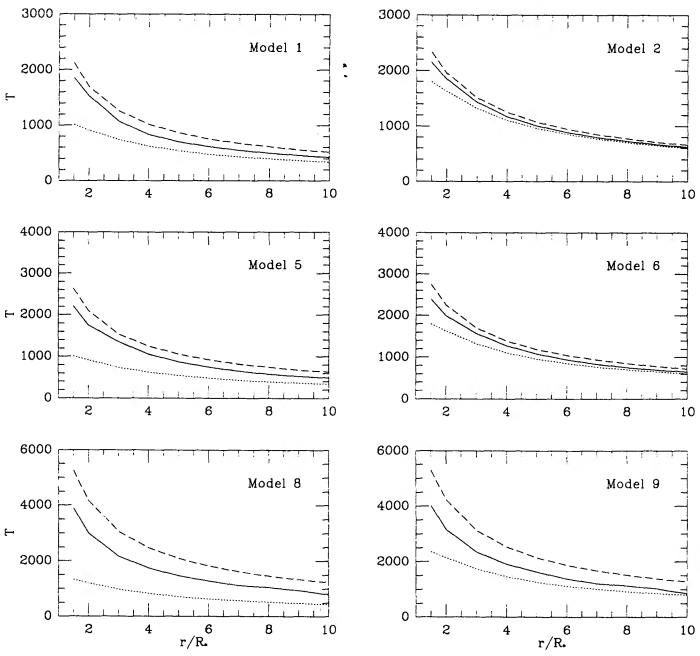

FIG. 4.—Disk effective temperature as a function of radius, for models 1, 2, 5, 6, 8, and 9 in Table 2. The plots are arranged so that the mass accretion rate increases from left to right and the stellar effective temperature increases from top to bottom. The dotted line corresponds to the effective temperature when only the viscous flux is present, while the dashed line corresponds to the "reprocessing" effective temperature given by eq. (26).

ing the values of the radiative and the adiabatic gradients. We find that the disk atmospheres are generally stable against convection if $\dot{M}_a \lesssim 10^{-6}\ M_\odot\ \mathrm{yr}^{-1}$. Small convective regions develop around the region where $T \approx 1500$ K due to the artificial jump in opacity around that region. A better treatment of the transition between molecular and dust opacity should be made before exploring further the convective instability in disk atmospheres.

When assuming RE, we are ignoring the rate of viscous energy deposition, which although small is present throughout the atmosphere. To check for the importance of this effect, we have compared a posteriori at each atmospheric depth the viscous energy deposition per unit volume $dF_{\mathrm{vis}}/dz = 1.5\alpha_v \Omega p$ with the rate of stellar heating per unit volume $\alpha q \chi_{\mathrm{Ross}} \rho E_0\, e^{-q\tau_d/\mu_0}$. If the stellar heating dominates, then the mechanical heating term is not important in the energy equation and RE holds. If, on the other hand, the viscous heating is more important, then RE is not appropriate, and a self-consistent solution for the temperature and the radiation field should be found, solving the transfer equations and the energy equation with mechanical heating included. We find that stellar heating dominates for $\tau_d \gtrsim 10^{-4}$ to 10^{-3}, for $\dot{M}_a \lesssim 10^{-6}\ M_\odot\ \mathrm{yr}^{-1}$. Since the spectral features discussed in this work are formed at $\tau_d \gtrsim 10^{-2}$, then they would not be significantly affected if the outer atmospheric structure were different. However, the predominance of viscous dissipation at high atmospheric levels may lead to an additional temperature rise, as already pointed out by Shaviv & Wehrse (1986) and Adams et al. (1988). Future treatments of the problem must include this effect.

A further assumption used in this work is that stellar rays reach the outer disk radii without being attenuated by the intervening gas. To check the validity of this assumption, we have calculated for a few cases the optical depth along a given ray (described by the angle $\cos^{-1}\mu_0$) for different disk radii. We find that optical depths along rays for $r \lesssim 10R_*$ are $\lesssim 0.3$. The small values of the optical depth are due to the fact that above the atmosphere the density is given by $\rho(z) \approx \rho_{\mathrm{at}} \exp -[(z - z_{\mathrm{at}})/H_{\mathrm{at}}(T_0)]^2$, where z_{at} and ρ_{at} are the height and density evaluated at some reference level in the region where the temperature has attained its asymptotic value, and H_{at} is the scale height. Since H_{at} is small in comparison with the disk height [$H_{\mathrm{at}} \approx 4 \times 10^9 (r/R_*)^{3/2} (T_0/3000\ \mathrm{K})^{1/2} (M/M_\odot)^{-1/2}$ cm] the density falls quite steeply, and there is little absorbing material along the ray.

4.3. *Optical Depth of the Disk*

As mentioned in § 3.5, in this study we do not prove that the disks are optically thick. However, we may get an idea of the appropriateness of the optically thick hypothesis calculating a posteriori the viscous flux going through the atmospheric layers and checking if it is approximately constant. Table 4 gives the value of τ at which the integrated viscous flux (in the manner described in § 3.5) falls to 10% of its surface value, for different accretion rates and stellar temperatures. The value of the viscosity parameter, α_v, in equation (23) plays an important role in this estimate, since it determines the rate of change of the viscous flux. Disks with low irradiation rates, $T_* = 4000$ K, are thick for all values of α_v, except for the innermost region when $\alpha_v \gtrsim 0.1$. On the other hand, as the stellar temperature increases, disks become hotter, less opaque, and more extended; the viscous flux changes more rapidly with τ; and disks become thin according to the criterion used, except for very low values of the viscosity parameter. As the mass accretion rate increases, however, the viscous flux increases as a whole, so that the relative rate of change decreases, and disks become thicker. Clarke et al. (1990) estimate that to have a decline in luminosity comparable to that observed in FU Ori systems, the parameter α_v has to be $\approx 10^{-3}$. This, together with our results, seem to imply that disks are optically thick at least for low stellar effective temperatures, since FU Ori outbursts are supposed to be produced by a high rate of accretion onto a low-mass star (Hartmann & Kenyon 1985, 1987; Kenyon et al. 1988).

An alternative criterion for inferring the optical depth of the disk would be to check a posteriori if the mass column density of the atmosphere is less than the total surface density, which is given by

$$\Sigma = \frac{\dot{M}_a}{\alpha_v c_s H}\left[1 - \sqrt{\left(\frac{R_*}{r}\right)}\right]$$

TABLE 4

OPTICAL DEPTH WHERE F_{vis} FALLS TO 10% OF ITS TOTAL VALUE

		$\dot{M}_a$								
		10^{-8}			10^{-7}			10^{-6}		
T_* (K)	r/R_*	$\alpha = 10^{-3}$	10^{-1}	1	$\alpha = 10^{-3}$	10^{-1}	1	$\alpha = 10^{-1}$	10^{-1}	1
4000	1.5	>5	0.2	10^{-2}	>5	0.5	6×10^{-2}	>5	1.7	0.3
	3	>5	>5	>5	>5	1.3	1.2	>5	3	0.5
	5	>5	>5	>5	>5	>5	>5	>5	0.7	0.2
	7	>5	>5	>5	>5	>5	>5	>5	1.5	1.5
	10	>5	>5	>5	>5	>5	>5	>5	>5	4.8
5000	1.5	>5	10^{-2}	5×10^{-5}	>5	0.5	10^{-2}	>5	1.77	0.2
	3	>5	10^{-2}	2×10^{-3}	>5	0.2	3×10^{-2}	>5	2.9	0.4
	5	>5	>5	>5	>5	>5	>5	>5	0.8	0.1
	7	>5	>5	>5	>5	>5	>5	>5	1.5	1.4
	10	>5	>5	>5	>5	>5	>5	>5	>5	4.7
10000.....	1.5	>5	2×10^{-2}	3×10^{-4}	>5	0.6	0.2	>5	>5	0.4
	3	>5	3×10^{-3}	8×10^{-5}	>5	0.5	2×10^{-3}	>5	3.5	0.1
	5	>5	4×10^{-4}	2×10^{-5}	>5	0.1	4×10^{-4}	>5	4	0.3
	7	>5	2×10^{-4}	6×10^{-6}	>5	4.2	2×10^{-4}	>5	2	0.1
	10	>5	5×10^{-5}	3×10^{-6}	>5	>5	4×10^{-5}	>5	1	1

TABLE 5

ABSORPTION EQUIVALENT WIDTH OR EMISSION FLUXES FOR THE $v = 2$–0 BAND HEAD

	W_λ(Å)			F^a (ergs cm^{-2} s^{-1})			$F_{2.93}{}^a$ (Jy)
Model	$i = 0°$	45°	80°	$i = 0°$	45°	80°	$i = 0°$
1.....	3.4	5.3	6.8	...	...	...	0.8
2.....	7.0	5.3	6.3	...	...	...	1.3
3.....	14.9	7.8	6.7	...	...	...	5.6
4.....	15.8	9.7	8.8	...	...	...	223.3
5.....	...	0.2	3.0	8.4×10^{-13}	...	...	1.5
6.....	0.4	1.7	3.1	...	...	...	1.9
7.....	12.0	6.1	4.5	...	...	...	6.0
8.....	...	...	...	1.5×10^{-10}	6.7×10^{-11}	8.9×10^{-12}	6.0
9.....	...	...	...	1.5×10^{-10}	6.6×10^{-11}	8.8×10^{-12}	7.4
10.....	...	...	...	1.1×10^{-10}	5.5×10^{-11}	7.6×10^{-12}	19.2
11.....	4.3	0.6	0.2	...	...	...	89.2
12.....	...	...	4.8	1.5×10^{-12}	2.2×10^{-13}	...	0.7
13.....	...	...	1.6	3.8×10^{-12}	2.9×10^{-13}	...	0.9

[a] Fluxes calculated at $d = 160$ pc.

(Shakura & Sunyaev 1973). For a given value of $\dot{M}_a$, the value of α_v sets the total surface density. Disks with a high value of α_v are more likely to be thin, while the larger $\dot{M}_a$, the higher the value of $\sum$ and the larger the optical depth, considerations which are in agreement with the previous results.

4.4. *Effect of Irradiation on the Intensity Emitted by the Disk*

The near-infrared intensity at each annuli of the disk and the flux of the star-disk system has been calculated for all models in Table 2. Table 5 gives either the equivalent width of the $v = 2$–0 band head in Å, if the band is in absorption, or the flux in this band head (in ergs cm^{-2} s^{-1} at 160 pc), if the band is emission, for each model. The theoretical equivalent width has been calculated between 2.293 and 2.305 μm, and the emission fluxes between 2.293 and 2.317 μm, to facilitate the comparison with Carr's (1989) observations discussed in the next section. The continuum flux at 2.293 μm at zero inclination is also given. It should be noted again that these fluxes have been calculated for a microturbulent velocity equal to the local sound velocity. Different values of the turbulent velocities would result in different values for the flux. Fluxes in Table 5 are meant to be illustrative, while the turbulent velocity should be taken as a parameter when fitting the spectrum of an individual object. Low-resolution spectra ($R = 1000$) for the cases in which the CO bands appear in emission are shown in Figure 5.

Molecular features are present in the spectrum of the disk atmosphere whenever its temperature is between $\approx$1500 and 4000 K (below 1500 K dust opacity dominates, while for temperatures higher than 4000 K, molecules are mostly dissociated). The strongest molecular bands in the near infrared are the vibrational-rotational bands of the ground electronic state of CO, although the H_2O bands and TiO band system are also present. For $\dot{M}_a \lesssim 10^{-6}\ M_\odot\ \mathrm{yr}^{-1}$ and low irradiation rates, most of the contribution to the near-infrared molecular spectrum of the disk comes from the innermost region, $r \lesssim 5R_*$, since it is in this region where temperatures are within the range in which molecular features appear. In the case of high irradiation rates, molecular bands are formed in a larger disk region, because all temperatures increase (see Table 3).

As discussed in § 3.1, one of the effects of irradiation from the stellar source on the disk atmosphere is to increase the temperature of the upper layers. If the surface temperature is lower than the effective temperature, the strong molecular features that form in the outermost regions appear in absorption. The absorption, however, is weaker than in the viscous disk atmosphere because of the higher surface temperatures. On the other hand, if the surface temperature is higher than the effective temperature, the bands appear in emission.

In the case of $T_* = 4000$ K and $\dot{M}_a \lesssim 10^{-8}\ M_\odot\ \mathrm{yr}^{-1}$, the surface temperature is higher than the effective temperature and above 1500 K for $r \lesssim 2R_*$ (see Table 3). At these radii, the strong CO bands are formed in the uppermost atmospheric regions and therefore are in emission in the disk spectrum. Weaker features, such as the bands of H_2O and TiO, are formed in deeper regions of the atmosphere of the inner disk

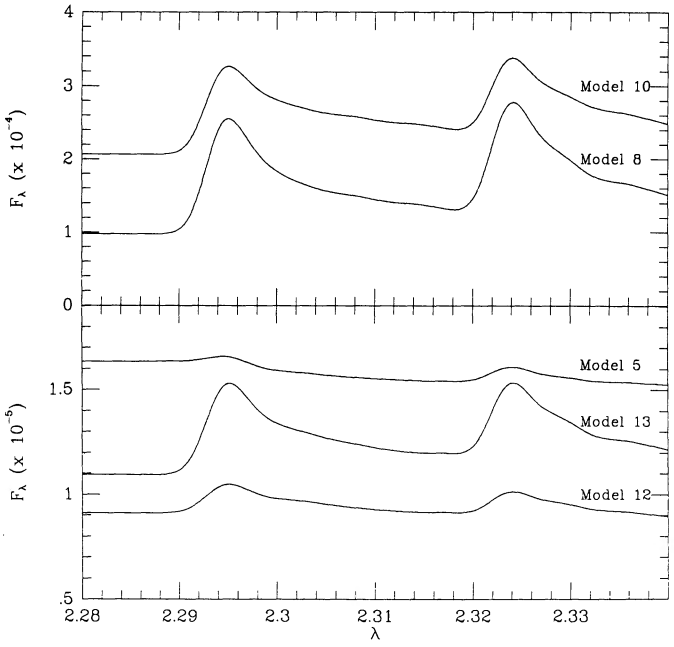

FIG. 5.—Low-resolution spectra ($R = 1000$) of the star-disk system in the 2–0 and 3–1 vibrational-rotational band of CO for cases where the CO bands appear in emission. Spectra are shown at an inclination of 45° and are identified by the model number in Table 2. Fluxes are calculated at a distance of 100 pc. Wavelengths are in microns and fluxes in ergs cm^{-3} s^{-1}.

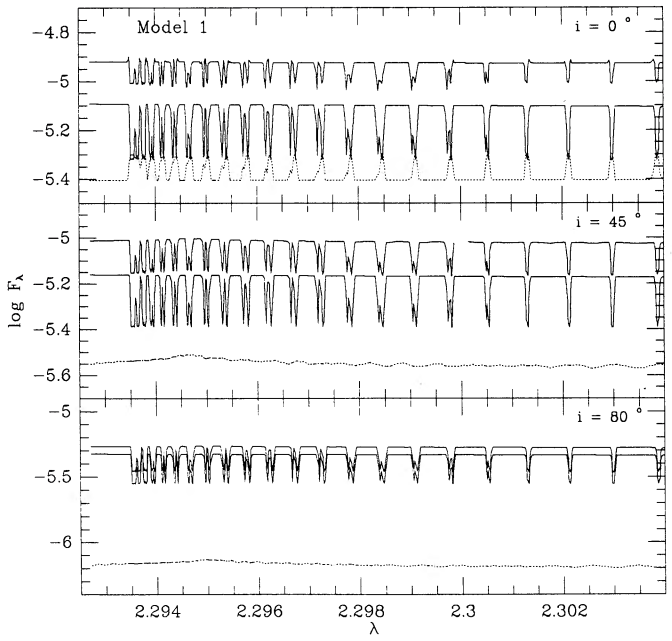

FIG. 6*a*

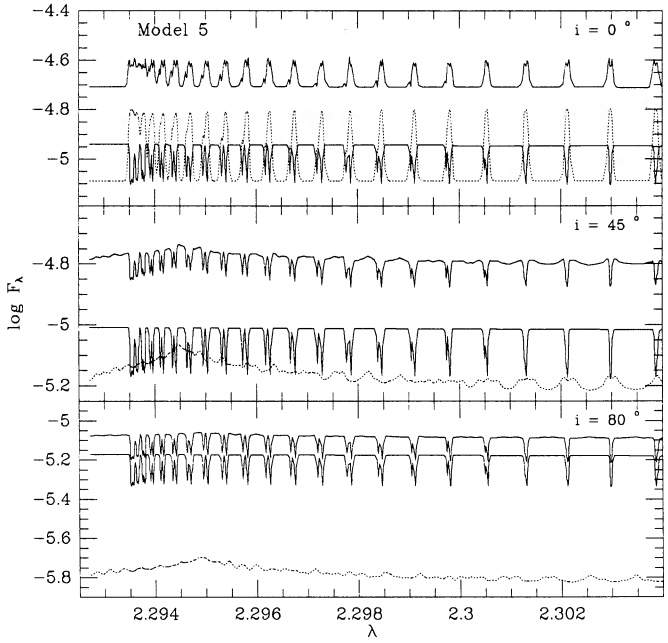

FIG. 6*b*

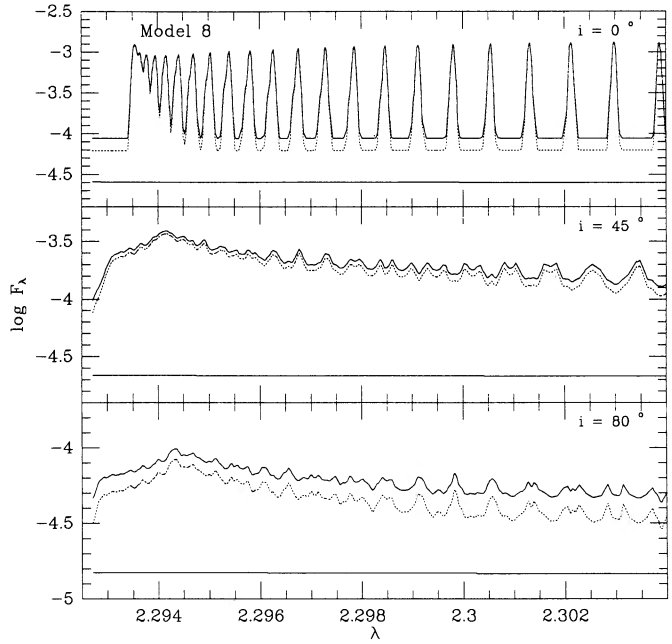

FIG. 6*c*

FIG. 6.—High-resolution spectra of the star-disk system in the 2–0 vibrational-rotational band of CO. Spectra are shown for inclinations $i = 0°$, 45°, and 80°, and for models with $\dot{M}_a = 10^{-8}\ M_\odot\ \mathrm{yr}^{-1}$ and increasing T_* in Table 2: (*a*) model 1, (*b*) model 5, (*c*) model 8. In most cases, the maximum radius is $R_{\max} = 10\ R_*$. The lower continuous line corresponds to the spectrum of the photosphere, while the upper corresponds to the spectrum of the star-disk system. The dotted line corresponds to the spectrum of the disk. Note the different scales in each graph. Microturbulence has been taken as the local sound velocity in these calculations. Wavelengths are in microns and fluxes are in ergs cm^{-3} s^{-1}. Fluxes are calculated at a distance of 100 pc.

and appear in absorption. However, in this case, the emergent spectrum of the star-disk system has the CO bands in absorption because the disk emission is not enough to compensate for the intrinsic absorption of the photosphere. Nevertheless, the CO bands are weaker than the photospheric bands. Figure 6*a* shows the emergent spectrum of the star-disk system for model 1 in Table 2, which has $\dot{M}_a = 10^{-8}\ M_\odot\ \mathrm{yr}^{-1}$ and $T_* = 4000$ K. The spectral interval shown covers the region corresponding to the $v'' - v' = 2$–0 band of the vibrational-rotation transitions of the ground electronic state of CO and is given for three disk inclinations, $i = 0°$, 45°, and 80°. The spectra of the disk and of the photosphere are also shown for comparison. It can be seen that although the CO bands are weakly in emission at $i = 0°$, the disk flux is much lower than the photospheric one and acts only as a source of veiling. As inclination increases, the disk contribution becomes weaker, since the projected emitted area decreases, and the spectrum of the system becomes increasingly similar to that of the photosphere. In the inner regions of disks with $\dot{M}_a \gtrsim 10^{-7}\ M_\odot\ \mathrm{yr}^{-1}$ and $T_* = 4000$ K, the disk effective temperature is of the order or larger than the surface temperature (see Table 3) and CO absorption features will form in the disk photosphere. The range of radii in the disk where CO forms increases and moves outwards as the mass accretion rate increases, following the increase of $T(r)$ with $\dot{M}_a$.

Figure 6*b* shows spectra for model 5 in Table 2, corresponding to $\dot{M}_a = 10^{-8}\ M_\odot\ \mathrm{yr}^{-1}$ and $T_* = 5000$ K. Since the disk is irradiated by a hotter star and therefore surface temperatures are higher, the disk emission features are stronger than in the lower stellar effective temperature case. At the same time, the intrinsic photospheric features are weaker, with the result that the bands appear in emission in the spectrum of the system. As inclination increases, each line is split into two weaker components with mean separation of twice the Doppler shift corresponding to the maximum orbital velocity, corrected by inclination. The double peak profile is not readily apparent in Figure 6, because the separation between lines is of the same order as the velocity shift between the peaks of each line, ≈ 0.001 μm for rotational velocities of ≈ 150 km s^{-1}. Components of different lines are then superposed and individual lines cannot be clearly discerned in the resultant inclined disk spectrum. Since lines become weaker and the projected area decreases, the disk contribution to the total spectrum decreases

with inclination relative to the photosphere and the bands appear in absorption at large inclinations.

In contrast, bands always appear in emission for high stellar temperatures. Figure 6*c* shows the spectrum of model 8 in Table 8, with $\dot{M}_a = 10^{-8}\ M_\odot\ \mathrm{yr}^{-1}$ and $T_* = 10{,}000$ K. The disk spectrum is stronger than that of the photosphere because of the high surface temperatures (Table 3) and larger emitting area. The region in the disk where the CO features form is larger, in comparison to the low irradiation rate case. For model 8, for instance, approximately the innermost $30R_*$, which corresponds to 90 $R_\odot$, contribute to the CO emission. The system spectrum is therefore in emission, although again the detailed structure of the band is washed out by rotation at high inclinations. In fact, emission will be present even for high $\dot{M}_a$; only for $\dot{M}_a \gtrsim 10^{-5}\ M_\odot\ \mathrm{yr}^{-1}$ the CO bands turn into absorption in the spectra of the irradiated disk.

5. DISCUSSION

According to the results of § 4, irradiation by the central star increases the temperature of the disk atmosphere relative to the case where only the viscous flux goes through it. The details of the temperature profile depend on the irradiation flux and on the viscous flux, which in turn can be described in terms of the stellar effective temperature and the mass accretion rate, respectively. For T_* small, $q \gtrsim 1$ (see Fig. 1), which means that the depth where $\tau \approx 1$ for the stellar radiation is located deep in the atmosphere and even the deepest layers are heated by the stellar radiation. As T_* increases for given $\dot{M}_a$ so does q, and an increasing fraction of the stellar energy is deposited in high atmospheric layers. As a result, as T_* increases, the surface temperature increases more rapidly than the effective temperature does and eventually becomes larger. Features formed in the outer layers, like the CO first-overtone bands, will then go into emission. On the other hand, as $\dot{M}_a$ increases for given T_*, the effective temperature increases more than the surface temperature does, and above a certain value of the mass accretion rate, the CO bands will appear in absorption. These considerations suggest that we can define regions in the (T_*, $\dot{M}_a$) plane in which one would expect either emission or absorption of the CO bands for the case of optically thick, steady accretion disks around young objects. These regions are shown in Figure 7, in which we have marked the intermediate region around which we expect to find no features with a dashed line.

For central stars with low effective temperature, $\lesssim 4000$ K, one expects to see the near infrared bands of CO in absorption, for $\dot{M}_a \gtrsim 10^{-8}\ M_\odot\ \mathrm{yr}^{-1}$. For low mass accretion rates, essentially the stellar absorption bands are seen, but they appear weaker than in the star because they are veiled by the disk continuum and line emission from the inner $\approx 2R_*$ in the disk. As the mass accretion rate increases, the disk effective temperature increases and band absorption in the inner disk becomes stronger and dominates over the photospheric bands.

When the temperature of the central star increases, disks with low $\dot{M}_a$ show the CO bands in emission (although if $\dot{M}_a$ is very low, the disk flux would be too low to be seen). As $\dot{M}_a$ increases, the emission bands become weaker, and after crossing the dividing line they turn into weak absorption. The strong CO absorption bands are expected only in cases of high $\dot{M}_a$. The value of $\dot{M}_a$ from where absorption bands are expected at given T_* increases with T_*. For stars with $T_* \gtrsim 10{,}000$ K, the mass accretion rate in the disk has to be $\gtrsim 10^{-5}\ M_\odot\ \mathrm{yr}^{-1}$ for the effective temperature to be high enough that the bands appear in absorption.

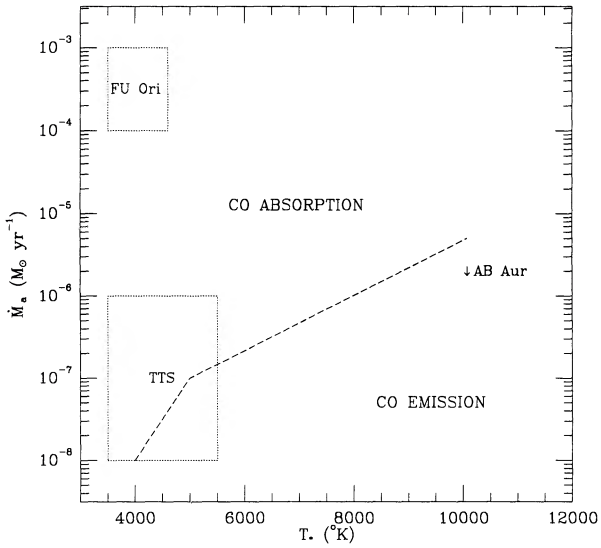

FIG. 7.—Mass accretion rate vs. stellar effective temperature. The dashed line separates the regions in which CO is expected to be either in absorption or in emission. The dotted lines encircle the regions where FU Ori objects and where T Tauri stars are found in this diagram. The arrow marks an upper limit for the mass accretion rate of the star AB Aur (see § 5 for details).

Observations confirm these predictions. The CO bands are strongly in absorption in the FU Ori objects (Mould et al. 1978; Carr 1989), which are thought to be stars previously appearing as T Tauri stars (so that $T_* = 4000$ K, $M_* \approx 1\ M_\odot$, $R_* \approx 3\ R_\odot$), surrounded by an accretion disk in which the mass accretion rate has increased to values 10^{-4} to $10^{-3}\ M_\odot\ \mathrm{yr}^{-1}$ (Hartmann & Kenyon 1985, 1987; Kenyon et al. 1988). In Figure 7 we show that the FU Ori objects fall in a region in which, according to our study, strong band absorption is expected. For a quantitative comparison, we have calculated the spectrum for an "FU Ori model" (model 4, see Table 2); for this model the equivalent width of the 2–0 band is between 16 and 10 Å, for inclinations between 0° and 45°, range in which the equivalent widths in FU Ori objects are observed. This agreement, in fact, also supports the disk interpretation for these type of objects, since another one of its predictions agrees with observations.

In Figure 7 we have marked the region in which T Tauri stars (TTS) are found. In this case, the estimate of mass accretion rate comes from the studies of emission from the boundary layer (KH; Bertout et al. 1988; Basri & Bertout 1989). From the location of TTS in the (T_*, $\dot{M}_a$) plane one would expect on statistical grounds absorption in the CO bands for most of them, which is indeed the case. In Carr's (1989) sample, 50% of the T Tauri stars show absorption, 15% show emission, and the rest are featureless within the detection limit. In fact, Carr's stars were chosen among those showing strong emission characteristics, and particularly, many of them are "continuum" stars, that is, stars with no photospheric absorption features; this veiling has been interpreted as due to the emission of the boundary layer. The boundary layer luminosities for these objects suggest $\dot{M}_a \approx 10^{-7}$ to $10^{-6}\ M_\odot\ \mathrm{yr}^{-1}$ (KH; Bertout et al. 1988; Basri & Bertout 1989), while continuum stars are generally assigned a late spectral type (K7, $T_* \approx 4000$ K). With these parameters, CO absorption would be expected for the continuum stars, and indeed, 70% of them show absorption, in agreement with our expectations. For $\dot{M}_a = 10^{-8}\ M_\odot\ \mathrm{yr}^{-1}$, the equivalent widths in Table 5 are 3 Å for $i = 0°$ and 7 Å for

$i = 80°$, weaker than the photospheric equivalent width of 7.5 Å. As discussed above, veiling by line and continuum emission by the atmosphere of the inner disk reduces the equivalent width of the system relative to the stellar one.

Two of the continuum stars in Carr's sample show emission in the CO near-infrared bands, namely, DG Tau and AS 353A. The emission of DG Tau has also been observed by Hamann, Simon, & Rydgway (1988). One could argue that these stars have higher effective temperature than the "typical" TTS. No absorption-line spectrum has been detected in AS 353A (Herbig & Bell 1988), but there are indications that DG Tau has a late type spectrum (Herbig 1977; Strom et al. 1986), close to early M. No emission would then be expected according to our results. We have not included in our treatment, however, the effect of irradiation by the boundary layer, which as mentioned above is thought to be responsible for the veiling that hides the photospheric absorption lines in the continuum stars. If the vertical height of the boundary layer is similar to that of the neighboring disk, then for geometrical reasons no effect is expected on the inner disk. However, if the boundary layer has some vertical extent over the equatorial part of the star, then irradiation by it can be significant in the inner disk, $r \lesssim 1.5$–$2\ R_*$ (Smak 1989). The boundary layer would act as a small but hot source, which in our treatment could be simulated by having E_0 comparable to that of a star of $T_* = 4000$ K but with q corresponding to a much higher temperature. The first assumption comes from the fact that the quantity L_{bl}/L_*, where L_{bl} is the boundary layer luminosity and L_* is the stellar luminosity, is of order unity for the continuum stars (Basri & Bertout 1989; L. Hartmann, private communication), and in particular for DG Tau, $L_{bl}/L_* \approx 2$; the second, from the temperatures that have been estimated for the boundary layer (KH; Bertout et al. 1988; Basri & Bertout 1989). We have calculated two "boundary layer" models (see Table 2) with E_0 equal to 1 and 2 times that of a star of $T_* = 4000$ K and q appropriate to $T = 10{,}000$ K. The CO bands turn into emission, as expected, with a band head flux given in Table 5. The continuum flux at 2.93 μm is also given in Table 5. The observed band flux of DG Tau is 8.7×10^{-13} ergs cm^{-2} s^{-1} and the observed continuum flux is 1.3 Jy (Carr 1989); comparison with fluxes predicted by the "boundary layer" models suggests that this is a viable explanation for the origin of the emission, although a more refined calculation must be done once the actual geometry of the boundary layer is known. In this context, it is interesting to notice that the observed equivalent width of the absorption bands in the continuum stars is 1–4 Å (Carr 1989), while the theoretical equivalent widths in Table 5 are larger. The theoretical equivalent width of the CO band head in the $T_* = 4000$ K model photosphere is 7.5 Å, as mentioned above, similar to the equivalent width of ≈ 8 Å for an M0 V star in the compilation of Kleinmann & Hall (1986). The intrinsic photospheric spectrum is then appropriate, and that cannot be the reason for the difference. A possible explanation would be that irradiation by the boundary layer makes the surface temperature in the disk higher than that expected in models where this additional effect is not included. The CO bands would then have a larger emission flux in the disk spectrum, so that in the spectrum of the star-disk system the photospheric bands would be even more veiled than in the case with no boundary layer. Eventually, if the effect of boundary layer irradiation is important enough, disk emission would dominate and the bands would appear in emission in the spectrum of the system.

Among the TTS with observed near-infrared spectra, there are three stars with well-defined spectral type, namely T Tau (KH), SU Aur, and CW Tau (Carr 1989). These stars have effective temperatures between 4500 and 5500 K (Cohen & Kuhi 1979), and their near-infrared spectrum around the CO bands is featureless within the observational uncertainties. According to our results these stars should have $5 \times 10^{-8} < \dot{M}_a < 5 \times 10^{-7}\ M_\odot$ yr^{-1}, in which case the atmospheric temperature would be almost constant (see Fig. 2) and the bands would be absent or only weakly in emission or absorption. Mass accretion rates have not been estimated for all of them, but for the case of T Tau (spectral type K1 V), KH determine from the ultraviolet excess $\dot{M}_a \approx 2 \times 10^{-7}\ M_\odot$ yr^{-1} (for an assumed mass of 2 $M_\odot$), which puts the star very near the dividing line between the absorption and emission regions in Figure 7, confirming our expectation.

Observations of the hot star AB Aur are also in agreement with theoretical expectations. The near-infrared spectrum of AB Aur shown in Hartmann et al. (1989) indicate that the CO bands are either absent or too weak to be detected with the instrument used. The spectral type of this star is B9–A0 (Cohen & Kuhi 1979), so that $T_* \approx 10{,}000$ K and from the weakness of the band, one would expect that the star were close to the dividing line in the $(T_*, \dot{M}_a)$ plane. For this, the mass accretion rate in the disk should be $1 \times 10^{-6} \lesssim \dot{M}_a < 1 \times 10^{-5}\ M_\odot$ yr^{-1}, according to Table 5 and Figure 7. Rydgren & Zak (1987) have estimated that the infrared excess luminosity above that expected from the star alone is $\lesssim 0.47 L_*$. If we assume that this excess luminosity comes from an accretion disk and take stellar parameters corresponding to a A0 V star (suggested by the similarity of the stellar luminosity with that of a main-sequence star), then we get $\dot{M}_a \lesssim 3 \times 10^{-6}\ M_\odot$ yr^{-1}. This excess luminosity has been attributed to stellar radiation reprocessed by a flaring disk, since the excess is less than $0.5 L_*$, the upper limit for the emission of a reprocessing, flaring disk (KH). In the treatment of KH, however, the assumptions of $q = 1$ and $\alpha = 1$ which lead to equation (26) were used. However, for the case $T_* \approx 10{,}000$ K, $q \gtrsim 10$ and $\alpha \lesssim 0.1$ for the range of temperatures involved (see Fig. 1). As a consequence, $(T_{rep} - T_{eff})/T_{rep}$ is $\approx 30\%$ for $\dot{M}_a = 10^{-8}\ M_\odot$ yr^{-1}, and $\approx 1\%$–10% for $\dot{M}_a = 10^{-6}\ M_\odot$ yr^{-1} (see Table 3); the continuum flux from the disk with a low mass accretion rate would then be lower than that calculated using equation (26). At $\lambda = 2.3$ μm, a model with $\dot{M}_a = 10^{-8}\ M_\odot$ yr^{-1} and $T_* = 10{,}000$ K (model 8) gives $\lambda F_\lambda = 8 \times 10^{-9}$ ergs cm^{-2} s^{-1} at 160 pc, while a model with $\dot{M}_a = 10^{-6}\ M_\odot$ yr^{-1} (model 10) gives $\lambda F_\lambda = 1.8 \times 10^{-8}$ ergs cm^{-2} s^{-1}, in much better agreement with the observed flux for AB Aur, $\lambda F_\lambda = 2 \times 10^{-8}$ ergs cm^{-2} s^{-1} (Rydgren & Zak 1987).

According to our results, it is more likely that the CO near-infrared bands appear in emission than in absorption in hot stars, whether the disks are optically thick, as in here, or optically thin (Carr 1989). One way to discriminate between the two possibilities is to consider the *continuum* infrared excess of the configuration, since if the disk is optically thin, then the expected continuum flux is lower than in the optically thick case. This indicates that in order to determine the actual nature of the accretion disk around a hot object from the near-infrared CO emission, both the flux in the bands and in the continuum must be considered.

We would like to thank the following for their comments

and suggestions to this work: Lee Hartmann, Scott Kenyon, Jorge Cantó, Luc Binette, and Alex Raga. G. M. C. has been supported by a fellowship from Fundación Gran Mariscal de Ayacucho. P. D. has been supported by a fellowship from Fundación Polar. Part of this work has been supported by Project No. C-380-89 of the CDCH of the Universidad de Los Andes and by the International Exchange Program of the Smithsonian Institution.

REFERENCES

Adams, F. C., Lada, C. J., & Shu, F. H. 1987, ApJ, 312, 788
Adams, J., Storzer, H., Shaviv, G., & Whehrse, R. 1988, A&A, 193, L1
Alexander, D. R., Augason, G. C., & Johnson, H. R. 1989, ApJ, 345, 1014
Alexander, D. R., Johnson, H. R., & Rypma, R. L. 1983, ApJ, 272, 773
Auman, J., Jr., 1967, ApJS, 14, 171
Basri, G., & Bertout, C. 1989, ApJ, 341, 340
Bertout, C. 1989, ARA&A, 27, 351
Bertout, C., Basri, G., & Bouvier, J. 1988, ApJ, 330, 350
Calvet, N., Magris, C. G., Patiño, A., & D'Alessio, P. 1991, Rev. Mexicana Astr. Af., submitted
Carbon, D. F., & Gingerich, O. 1969, in Theory and Observations of Normal Stellar Atmospheres, ed. O. Gingerich (Cambridge: MIT Press), 377
Carr, J. S. 1989, ApJ, 345, 522
Clarke, C. J., Lin, D. N. C., & Pringle, J. E. 1990, MNRAS, 242, 439
Cohen, M., & Kuhl, L. V. 1979, ApJ, 41, 743
Collins, J. G., & Fay, T. D. Jr. 1974, J. Quant. Spectrosc. Rad. Transf., 14, 1259
Dalgarno, A. 1962, Spectral Reflectivity of the Earth's Atmosphere. III. The Scattering of Light by Atomic Systems. Geophys. Corp. of America, GCA Tech. Rep. 62-28-A.
Draine, B. T. 1987, Princeton Observatory preprint, 213
Draine, B. T., & Lee, H. M. 1984, ApJ, 285, 89
Gray, D. F. 1976, The Observation and Analysis of Stellar Photospheres (New York: Wiley)
Hamann, F., Simon, M., & Ridgway, S. T. 1988, ApJ, 326, 859
Hartmann, L. W., & Kenyon, S. J. 1985, ApJ, 299, 462
———. 1987, ApJ, 312, 243
———. 1988, ApJ, 325, 231
Hartmann, L. W., Kenyon, S. J., Hewett, R., Edwards, S., Strom, K. M., Strom, S. E., & Stauffer, J. R. 1989, ApJ, 338, 1001
Herbig, G. H. 1977, ApJ, 217, 693
———. 1989, in Low Mass Star Formation and Pre-Main-Sequence Objects, ESO Workshop, ed. B. Reipurth (Garching: ESO), 233
Herbig, G. H., & Bell, K. R. 1988, Lick Obs. Bull., 1111
Kenyon, S. J., & Hartmann, L. W. 1987, ApJ, 323, 714 (KH)
Kenyon, S. J., Hartmann, L. W., & Hewett, R. 1988, ApJ, 325, 231
Kirby-Docken, K., & Liu, B. 1978, ApJS, 36, 359
Kleinmann, S. G., & Hall, D. N. B. 1986, ApJS, 62, 501
Kurucz, R. L. 1970, SAO Spec. Rept., 309
Ludwig, C. B., Malkmus, W., Reardon, J. E., & Thompson, J. A. L. 1973, Handbook of Infrared Radiation from Combustion Gases (NASA SP-3080)
Lynden-Bell, D., & Pringle, J. E. 1974, MNRAS, 168, 603
McDowell, M. R. C., Williamson, J. H., & Myerscough, V. P. 1966, ApJ, 144, 827
Mihalas, D. 1967, in Methods in Computational Physics, ed. B. Alder, S. Fernbach, & M. Rotenberg (New York: Academic), 1
———. 1978, Stellar Atmospheres (San Francisco: Freeman)
Milne, E. A. 1930, Handbuch der Astrophysik, 3, 65
Mould, J. R., Hall, D. N. B., Ridgway, S. T., Hintzen, P., & Aaronson, M. 1978, ApJ, 222, L123
Rydgren, A. E., & Zak, D. S. 1987, PASP, 99, 141
Scoville, N., Kleinmann, S. G., Hall, D. N. B., & Ridgway, S. T. 1983, ApJ, 275, 201
Shakura, N. I., & Sunyaev, R. A. 1973, A&A, 24, 337
Shaviv, G., & Whehrse, R. 1986, A&A, 159, L5
Smak, J. 1989, Acta Astr., 39, 201
Strittmatter, P. A. 1974, A&A, 32, 7
Strom, K. H., Strom, S. E., Wolff, S. C., Morgan, J., & Wenz, M. 1986, ApJS, 62, 39
Tatum, J. B. 1966, Pub. Dom. Ap. Obs., 13, 1
Thompson, R. I. 1985, ApJ, 299, L41
Thompson, R. I., Strittmatter, P. A., Erickson, E. F., Witteborn, F. C., & Strecker, D. W. 1977, ApJ, 218, 170
Tsuji, T. 1966, PASJ, 18, 127
———. 1969, Low Luminosity Stars, ed. S. S. Kumar (New York: Gordon & Breach), 457
Vardya, M. S. 1962, ApJ, 135, 303